

Cite this: *Chem. Commun.*, 2011, **47**, 10416–10418[www.rsc.org/chemcomm](http://www.rsc.org/chemcomm)

## COMMUNICATION

Spin crossover in the cyanide-bridged  $\text{Mo}^{\text{V}}\text{Mn}^{\text{III}}$  single-chain magnet containing  $\text{Fe}^{\text{II}}$  cations†Jung Hee Yoon,<sup>a</sup> Dae Won Ryu,<sup>a</sup> Sang Yup Choi,<sup>a</sup> Hyoung Chan Kim,<sup>b</sup> Eui Kwan Koh,<sup>c</sup> Jun Tao<sup>d</sup> and Chang Seop Hong<sup>\*a</sup>

Received 18th June 2011, Accepted 27th July 2011

DOI: 10.1039/c1cc13627e

A 1D  $\text{Mo}^{\text{V}}\text{Mn}^{\text{III}}$  chain compound balanced by  $\{\text{Fe}[\text{HC}(3,5\text{-Me}_2\text{pz})_3]_2\}^{2+}$  dications was prepared. This complex displays a typical single-chain magnet character associated with the  $\text{Mo}^{\text{V}}\text{Mn}^{\text{III}}$  chain and a spin crossover phenomenon arising from cationic  $\text{Fe}(\text{II})$  subunits. The spin crossover behavior tends to slightly affect single-chain magnetic properties at low temperature.

Single-chain magnets (SCMs) are one of the current issues because of the fundamental interest and potential applications in magnetic devices. The intrinsic ingredients to achieve SCMs are generally regarded as anisotropic sources in a one-dimensional (1D) chain structure and negligible interchain magnetic interactions relative to intrachain couplings. A large number of 1D coordination polymers exhibiting a slow relaxation of magnetization have been demonstrated by means of several strategies.<sup>1</sup>

Spin crossover (SCO) is controlled readily by external stimuli such as temperature, pressure, light, or solvents.<sup>2</sup> This SCO property can be combined with other characters to display intriguing bifunctional features. A limited number of corresponding examples have been successfully demonstrated so far and, for instance, they possess not only the SCO trait but also spin glasses,<sup>3</sup> chirality,<sup>4</sup> conductivity,<sup>5</sup> long-range order,<sup>6</sup> or porosity to induce guest-sensitive SCO signals.<sup>7</sup> On the other hand, prospective open questions have arisen to pursue multifunctional SCMs.<sup>8</sup> Although some functional materials have been exemplified recently an example with SCM and SCO characters is still missing to date.<sup>9</sup>

To realize such a system one can design a 1D chain structure in which 1D chains are well separated by SCO units. This is because SCM characteristic demands ignorable interchain magnetic interactions while SCO behavior is established at a

molecular level. In this vein, we attempted to employ octacyano-metalate  $[\text{Mo}(\text{CN})_8]^{3-}$ , capable of constructing various structures,<sup>10</sup> and a  $\text{Mn}(\text{III})$  Schiff base with an anisotropic center as a chain building unit,<sup>11</sup> together with  $\{\text{Fe}[\text{HC}(3,5\text{-Me}_2\text{pz})_3]_2\}^{2+}$  (pz = pyrazolyl ring) as a SCO carrier.<sup>12</sup> In this communication, we present the synthesis, structures, and magnetic properties of 1D chains  $[\text{Mo}(\text{CN})_8\text{Mn}(5\text{-Brsalcy})]\{\text{M}[\text{HC}(3,5\text{-Me}_2\text{pz})_3]_2\} \cdot x(\text{solvents})$  [ $\text{M} = \text{Fe}$  (**1**:  $2\text{MeOH} \cdot 5\text{H}_2\text{O}$ ) and  $\text{Cd}$  (**2**:  $\text{H}_2\text{O}$ ); 5-Brsalcy = *N,N'*-(*trans*-1,2-cyclohexanediyethylene)bis(5-bromosalicylideneiminato) dianion]. The complex **1** marks the first example notably exhibiting concomitant SCM and SCO properties and the two characters are correlated to some extent.

Complexes **1** and **2** crystallize in the triclinic system with the space group  $P\bar{1}$ . In the crystal structures (Fig. 1 and Fig. S1, ESI†), the Mo center is a distorted dodecahedron consisting of eight C atoms from CN ligands (mean Mo–C length = 2.158(9) Å). The Mo–C–N angles are almost linear with a maximum deviation from 180° of 4° (**1**) and 3.8° (**2**). Each Mn atom adopts a distorted octahedron with a severe tetragonal elongation as judged by the longer axial Mn–N distances [Mn1–N1 = 2.322(5) Å, Mn1–N8a = 2.343(5) Å for **1** and Mn1–N1c = 2.330(7) Å, Mn1–N8 = 2.338(7) Å for **2**;  $a, c = -1 + x, y, z$ ] and the shorter equatorial Mn–N(O) distances ranging from 1.858 to 1.992 Å. This distortion is ascribed to the Jahn–Teller effect of an octahedral high-spin Mn(III) ion.<sup>13</sup> The Mn–N–C angles in the bridging routes for **1**

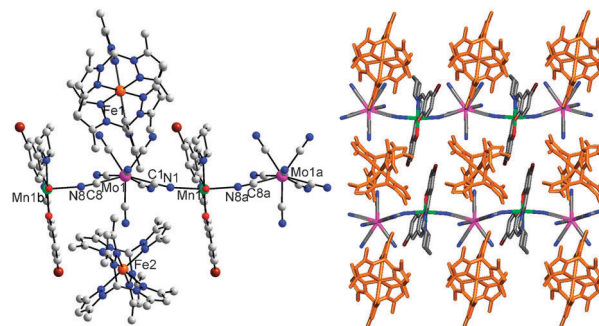


**Fig. 1** (left) Molecular view of **1**. Symmetry transformations were used to generate equivalent atoms:  $a = -1 + x, y, z$  and  $b = 1 + x, y, z$ . (right) Extended structure with 1D chains running along the *a*-axis and Fe moieties sitting between the chains.

<sup>a</sup> Department of Chemistry, Research Institute for Natural Sciences, Korea University, Seoul 136-713, Korea.

E-mail: [eshong@korea.ac.kr](mailto:eshong@korea.ac.kr)

<sup>b</sup> National Fusion Research Institute, Daejeon 305-333, Korea

<sup>c</sup> Nano-Bio System Research Team, Korea Basic Science Institute, Seoul 136-713, Korea

<sup>d</sup> Department of Chemistry, Xiamen University, Xiamen 361005, People's Republic of China

† Electronic supplementary information (ESI) available: Additional synthetic, structural, and magnetic details. CCDC 793931 (**1**) and 821662 (**2**). For ESI and crystallographic data in CIF or other electronic format see DOI: 10.1039/c1cc13627e

are 159.7(4)° for Mn1–N1–C1 and 167.4(4)° for Mn1–N8a–C8a, respectively, while those for **2** are almost identical to those for **1**, 158.4(7)° for Mn1–N1c–C1c and 167.6(9)° for Mn1–N8–C8. Two of eight CN groups in  $[\text{Mo}(\text{CN})_8]^{3-}$  bridge adjacent Mn Schiff bases, forming a linear 1D anionic chain  $[\text{Mo}(\text{CN})_8\text{Mn}(\text{5-Brsalcy})]^{2-}$  with intrachain distances of 5.542(1) Å for Mo1–Mn1 and 5.619(1) Å for Mn1–Mo1a (**1**), and 5.551(1) Å for Mo1c–Mn1 and 5.638(1) Å for Mn1–Mo1 (**2**). The organized chain requires cationic parts to maintain charge balance and then a  $\{\text{M}[\text{HC}(3,5\text{-Me}_2\text{pz})_3]_2\}^{2+}$  cation is inserted in the chain structure. In the cationic fragment, the M atom is sandwiched by two tridentate  $\text{HC}(3,5\text{-Me}_2\text{pz})_3$  ligands. The Fe–N bond length spans from 2.164 to 2.182 Å, which mainly belongs to the range of a high-spin Fe(II) state.<sup>14</sup> Since the existent bulky cationic entities are positioned in between  $\text{Mo}^{\text{V}}\text{Mn}^{\text{III}}$  chains, the 1D coordination polymers are separated from each other by the shortest interchain Mn–Mn distance of 10.629 Å (**1**) and 10.639 Å (**2**). The shortest Mo–M distances are still long, 8.695 Å for Mo1–Fe1 and 8.971 Å for Mo1–Fe2 (**1**), and 8.804 Å for Mo1–Cd1 and 8.907 Å for Mo1–Cd2 (**2**) (Fig. S2–S5, ESI†). The paramagnetic Fe monomers are isolated in the presence of Schiff bases and the shortest Fe–Fe distance is equal to 10.770 Å. Although there are many hydrogen bonds among lattice water molecules, MeOH, and unbound CN ligands in the crystal packing, the magnetic chains are well segregated owing to the long pathways through the hydrogen bonding. No  $\pi$ – $\pi$  contacts are detected in the structure.

The magnetic susceptibility data for **1** were collected at 1000 G and are depicted in Fig. 2a as a function of temperature. The  $\chi_{\text{m}}T$  product at 300 K equals  $7.38 \text{ cm}^3 \text{ K mol}^{-1}$ , which is compared with the spin-only value ( $6.38 \text{ cm}^3 \text{ K mol}^{-1}$ ) resulting from  $\text{Mo}^{\text{V}}$  ( $S_{\text{Mo}} = 1/2$ ),  $\text{Mn}^{\text{III}}$  ( $S_{\text{Mn}} = 2$ ), and high-spin  $\text{Fe}^{\text{II}}$  ( $S_{\text{Fe}}^{\text{hs}} = 2$ ). The larger experimental value may be a consequence of an orbital contribution of  $\text{Fe}^{\text{II}}$  ions because magnetic interactions among spin centers should be weak if any at room temperature in cyanide-bridged bimetallic systems.<sup>1,13,15</sup> Cooling the sample causes  $\chi_{\text{m}}T$  to decrease and reach a plateau at  $T < 60 \text{ K}$ . This flat propensity remains until  $T = 6 \text{ K}$ . Below that temperature,  $\chi_{\text{m}}T$  undergoes an abrupt rise to  $7.993 \text{ cm}^3 \text{ K mol}^{-1}$  at 2 K.

In the high- $T$  region of  $\chi_{\text{m}}T$  in **1**, the obvious anomaly, which is not seen in **2** with the diamagnetic  $\text{Cd}^{2+}$  ions

(Fig. S6, ESI†), implies that the signal stems solely from the Fe moieties. For the  $\{\text{Fe}[\text{HC}(3,5\text{-Me}_2\text{pz})_3]_2\}^{2+}$  fragment, the spin-crossover properties can be readily varied depending on the Fe(II) environments induced from the types of crystalline forms and anions.<sup>12</sup> Compared to the dicationic complex with a sharp SCO, the rather gradual and incomplete spin transition in **1**, which is referred to as a type e spin transition curve among the five representative types, may be due to the well-isolated Fe(II) moieties residing between the 1D chains built by  $\text{Mo}(\text{v})$  and  $\text{Mn}(\text{III})$  ions, which probably gives rise to an insufficient field strength for the low-spin state and a lack of cooperativity throughout the solid.<sup>16</sup>

From the simple upturn in  $\chi_{\text{m}}T$  of **1** at low temperatures, the underlying magnetic nature between Mo and Mn spins within a chain could not be concluded as either ferromagnetic or antiferromagnetic at this stage, because zero-field splitting, a contribution of the Fe ion, and magnetic interactions among magnetic spins in the lattice are mutually entangled in the low- $T$  regime. To elucidate the genuine magnetic coupling, the thermal variation of magnetic data of **2** in which diamagnetic  $\text{Cd}^{2+}$  ions are included instead of  $\text{Fe}^{2+}$  is inspected (Fig. S6, ESI†). The steady increase in  $\chi_{\text{m}}T$  evidences the operation of intrachain ferromagnetic interactions between Mo and Mn centers. The fit of the data with the Seiden chain model  $[\mathbf{H} = -2J\sum_i(\mathbf{S}_{\text{Mn}i}\mathbf{S}_{\text{Mo}i} + \mathbf{S}_{\text{Mn}i}\mathbf{S}_{\text{Mo}i+1})]$  under consideration of an interchain magnetic term ( $zJ'$ ) affords  $g = 1.95(1)$ ,  $J = 2.8(1) \text{ cm}^{-1}$ , and  $zJ' = 0.027(4) \text{ cm}^{-1}$ .<sup>17</sup> The magnetization value ( $4.44 N\beta$ ) in the  $M(H)$  curve is close to the intrachain ferromagnetic result between two spins (Fig. S7, ESI†). Comparison of structural parameters of Mn– $\text{N}_{\text{ax}}$  ( $\text{ax} = \text{axial}$ ) lengths, Mn– $\text{N}_{\text{ax}}$ – $\text{C}_{\text{ax}}$  angles, and Mo geometry suggests that the  $\chi_{\text{m}}T$  rise for **1** is pertinent to the occurrence of intrachain ferromagnetic couplings as for **2**. The spin density of the bridging N atoms is quite similar to each other, also supporting such a magnetic situation (Fig. S8, ESI†). The saturation magnetization of  $8.09 N\beta$  in **1** also indicates that, together with the Fe(II) contribution, the two dissimilar  $\text{Mo}(\text{v})$  and  $\text{Mn}(\text{III})$  spins in a chain are ferromagnetically coupled (inset of Fig. 2a).

To examine the underlying spin conversion in **1**, we measured pressure effects on magnetic properties (Fig. 2b). The SCO behaviors can be affected by pressure because the potential well of the high-spin state is subject to a vertical increase with respect to the original potential.<sup>18</sup> This scenario concurs with the observation of the pressure-induced spin state conversion in the current system. The  $\chi_{\text{m}}T$  value at  $P = 1 \text{ bar}$  and  $T = 10 \text{ K}$  is reduced by 38% at  $P = 1.7 \text{ kbar}$  and  $T = 10 \text{ K}$  due to the decrease of the high-spin Fe(II) fraction upon pressure.

To probe the spin dynamics of **1** and **2**, ac magnetic susceptibilities at zero dc field, an ac field of 5 G, and several oscillating frequencies ( $f$ ) were measured, as illustrated in Fig. 3, Fig. S9 and S10 (ESI†). An examination of the in-phase signals ( $\chi'_{\text{m}}$ ) shows that the maximum in  $\chi'_{\text{m}}$  shifts toward higher temperatures with increasing  $f$ . A quantity ( $\phi$ ), given by  $\Delta T_{\text{p}}/[T_{\text{p}}\Delta(\log f)]$ , was utilized to afford  $\phi = 0.19$  for **1** and 0.21 for **2**. These obtained values are out of range for canonical spin glasses and are consistent with a superparamagnet.<sup>1,19</sup> Clear frequency-dependent behavior was also observed in the out-of-phase component ( $\chi''_{\text{m}}$ ) and

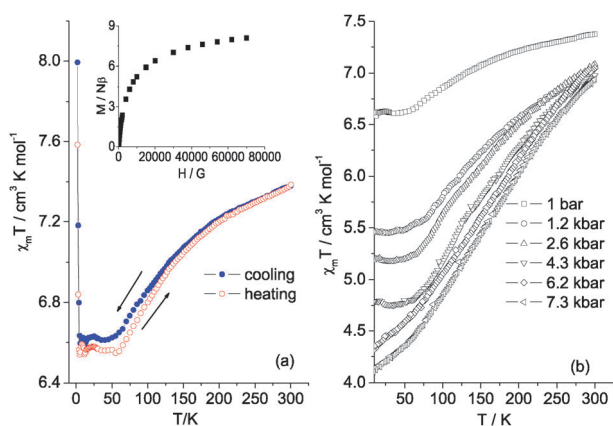


**Fig. 2** (a) Plots of  $\chi_{\text{m}}T$  versus  $T$  and  $M$  versus  $H$  (inset) per  $\text{MoMnFe}$  for **1**. (b) Plots of  $\chi_{\text{m}}T$  versus  $T$  at different pressures for **1**.

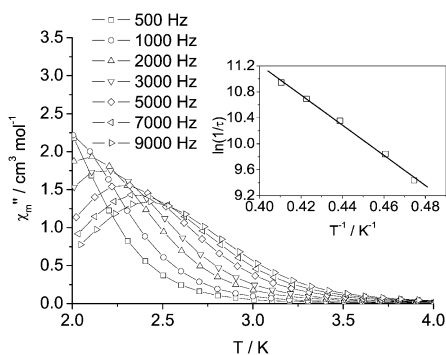


**Fig. 3** Temperature dependence of  $\chi_m''$  for **1** at several oscillating frequencies. Arrhenius plot for **1** is shown in the inset.

the Arrhenius formula  $\tau = \tau_0 \exp(\Delta_\tau/kT)$  where  $\tau = 1/2\pi f$  was applied to attain  $\tau_0 = 1.23 \times 10^{-9}$  s and  $\Delta_\tau = 16.1 \text{ cm}^{-1}$  for **1** (inset of Fig. 3), and  $\tau_0 = 7.29 \times 10^{-10}$  s and  $\Delta_\tau = 16.1 \text{ cm}^{-1}$  for **2** (Fig. S11, ESI†). The pre-exponential factor  $\tau_0$  falls in the usual range of normal SCMs.<sup>1,20</sup> The frequency dependence of ac data was collected at several temperatures (Fig. S12 and S13, ESI†) and the Cole–Cole diagrams at the identical temperatures are plotted in Fig. S14 (ESI†). A generalized Debye model was employed to fit the data, resulting in  $\alpha$  parameter values less than 0.21 for **1** and 0.22 for **2**. The  $\alpha$  values are indicative of a narrow distribution of single relaxation processes.

In the case of the Ising chain, at low temperature, the magnetic correlation length ( $\xi$ ) increases exponentially and the correlated magnetic segments are sectioned by domain walls.<sup>21</sup> To describe such 1D anisotropic situation at low temperatures, the  $\chi T$  product, proportional to the correlation length, can be expressed as  $\chi T = C_{\text{eff}} \exp(\Delta_\xi/kT)$  where  $\Delta_\xi$  is the energy barrier needed to create a domain wall in the chain. Based on this equation, a plot of  $\ln(\chi_m'' T)$  against  $1/T$  provides a straight line in a low-temperature range and a slope in the linear fit should correspond to the activation energy of the domain walls. The fitting process in the low- $T$  range ( $T < 6$  K) results in  $\Delta_\xi = 1.6 \text{ cm}^{-1}$  for **1** and  $6.5 \text{ cm}^{-1}$  for **2** (Fig. S15 and S16, ESI†). With reference to  $\Delta_\xi = 4JS_1S_2$ ,<sup>22</sup> the  $J$  value in the measured temperature region is expected to be  $0.4 \text{ cm}^{-1}$  for **1** and  $1.6 \text{ cm}^{-1}$  for **2** (smaller than the experimental value of  $2.8 \text{ cm}^{-1}$ , indicating a deviation from an Ising chain system). The intrachain magnetic coupling constant of **2** is greater than that of **1**. This is probably relevant to some degree of structural contractions in **1** triggered by SCO at low temperatures, which could lead to the local distortion of the bridging routes responsible for magnetic exchange coupling.

In summary, we have prepared and characterized 1D  $\text{Mo}^{\text{V}}\text{Mn}^{\text{III}}$  chain complexes containing  $\{\text{M}[\text{HC}(3,5\text{-Me}_2\text{pz})_2]_2\}^{2+}$  ( $\text{M} = \text{Fe}$  (**1**) and  $\text{Cd}$  (**2**)) cations. The complex with  $\text{M} = \text{Fe}$  is the first case remarkably exhibiting simultaneous SCM behavior attributed to the  $\text{Mo}^{\text{V}}\text{Mn}^{\text{III}}$  anisotropic chain and SCO feature associated with the  $\text{Fe}(\text{II})$  dication. It appears that the SCM properties are slightly perturbed by the involvement of SCO. From the synthetic strategy used in this system, it is envisioned that other dual functionalities may be readily obtained by substituting the SCO dication with other functional cations.

This work was supported by grants from the National Research Foundation of Korea funded by the Korean

Government (No. 2011-0003264) and by the Priority Research Centers Program through the National Research Foundation of Korea (NRF) funded by the Ministry of Education, Science and Technology (NRF20110018396).

## Notes and references

- H.-L. Sun, Z.-M. Wang and S. Gao, *Coord. Chem. Rev.*, 2010, **254**, 1081.
- M. Nihei, H. Tahira, N. Takahashi, Y. Otake, Y. Yamamura, K. Saito and H. Oshio, *J. Am. Chem. Soc.*, 2010, **132**, 3553.
- A. I. S. Neves, J. C. Dias, B. J. C. Vieira, I. C. Santos, M. B. C. L. Branco, C. J. Pereira, J. C. Waerenborgh, M. Almeida, D. Belo and V. Gama, *CrystEngComm*, 2009, **11**, 2160.
- Y. Sunatsuki, Y. Ikuta, N. Matsumoto, H. Ohta, M. Kojima, S. Iijima, S. Hayami, Y. Maeda, S. Kaizaki, F. Dahan and J.-P. Tuchagues, *Angew. Chem., Int. Ed.*, 2003, **42**, 1614.
- K. Takahashi, H.-B. Cui, Y. Okano, H. Kobayashi, H. Mori, H. Tajima, Y. Einaga and O. Sato, *J. Am. Chem. Soc.*, 2008, **130**, 6688.
- M. Arai, W. Kosaka, T. Matsuda and S. Ohkoshi, *Angew. Chem., Int. Ed.*, 2008, **47**, 6885.
- (a) P. D. Southon, L. Liu, E. A. Fellows, D. J. Price, G. J. Halder, C. K. W. Hapman, B. Moubarak, K. S. Murray, J.-F. Létard and C. J. Kepert, *J. Am. Chem. Soc.*, 2009, **131**, 10998; (b) M. Ohba, K. Yoneda, G. Agustí, M. C. Muñoz, A. B. Gaspar, J. A. Real, M. Yamasaki, H. Ando, Y. Nakao, S. Sakaki and S. Kitagawa, *Angew. Chem., Int. Ed.*, 2009, **48**, 4767; (c) B. Li, R.-J. Wei, J. Tao, R.-B. Huang, L.-S. Zheng and Z. Zheng, *J. Am. Chem. Soc.*, 2010, **132**, 1558; (d) M. Hostettler, K. W. Törnroos, D. Chernyshov, B. Vangdal and H.-B. Bürgi, *Angew. Chem., Int. Ed.*, 2004, **43**, 4589.
- (a) H. Miyasaka, M. Julve, M. Yamashita and R. Clérac, *Dalton Trans.*, 2009, 7331; (c) W. Ouellette, A. V. Prosvirin, K. Whitenack, K. R. Dunbar and J. Zubieta, *Angew. Chem., Int. Ed.*, 2009, **48**, 2140.
- (a) T. Liu, Y.-J. Zhang, S. Kanegawa and O. Sato, *J. Am. Chem. Soc.*, 2010, **132**, 8250; (b) C.-F. Wang, D.-P. Li, X. Chen, X.-M. Li, Y.-Z. Li, J.-L. Zuo and X.-Z. You, *Chem. Commun.*, 2009, 6940.
- (a) Y. S. You, D. Kim, Y. Do, S. J. Oh and C. S. Hong, *Inorg. Chem.*, 2004, **43**, 6899; (b) J. H. Lim, J. S. Kang, H. C. Kim, E. K. Koh and C. S. Hong, *Inorg. Chem.*, 2006, **45**, 7821; (c) Z.-X. Wang, X.-F. Shen, J. Wang, P. Zhang, Y.-Z. Li, E. N. Nfor, Y. Song, S.-i. Ohkoshi, K. Hashimoto and X.-Z. You, *Angew. Chem., Int. Ed.*, 2006, **45**, 3365.
- H. Miyasaka, A. Saitoh and S. Abe, *Coord. Chem. Rev.*, 2007, **251**, 2622.
- (a) D. L. Reger, C. A. Little, V. G. Young Jr. and M. Pink, *Inorg. Chem.*, 2001, **40**, 2870; (b) C. Piquer, F. Grandjean, O. Mathon, S. Pascarelli, D. L. Reger, C. A. Little and G. J. Long, *Inorg. Chem.*, 2003, **42**, 982; (c) D. L. Reger, C. A. Little, M. D. Smith, A. L. Rheingold, K.-C. Lam, T. L. Concolino, G. J. Long, R. P. Hermann and F. Grandjean, *Eur. J. Inorg. Chem.*, 2002, 1190; (d) D. L. Reger and C. A. Little, *Inorg. Chem.*, 2001, **40**, 1508.
- (a) J. I. Kim, H. S. Yoo, E. K. Koh, H. C. Kim and C. S. Hong, *Inorg. Chem.*, 2007, **46**, 8481; (b) J. H. Yoon, D. W. Ryu, H. C. Kim, S. W. Yoon, B. J. Suh and C. S. Hong, *Chem.–Eur. J.*, 2009, **15**, 3661.
- A. Hauser, *Adv. Polym. Sci.*, 2004, **233**, 49.
- B. Li, R. J. Wei, J. Tao, R.-B. Huang and L.-S. Zheng, *Inorg. Chem.*, 2010, **49**, 745.
- P. Gülich and H. A. Goodwin, *Top. Curr. Chem.*, 2004, **233**, 1.
- (a) J. Seiden, *J. Phys. Lett.*, 1983, **44**, 947; (b) T. D. Harris, C. Coulon, R. Clérac and J. R. Long, *J. Am. Chem. Soc.*, 2011, **133**, 123.
- V. Ksenofontov, A. B. Gaspar and P. Gülich, *Top. Curr. Chem.*, 2004, **235**, 23.
- J. A. Mydosh, *Spin Glasses: An Experimental Introduction*, Taylor & Francis, London, 1993.
- J. H. Yoon, J. W. Lee, D. W. Ryu, S. W. Yoon, B. J. Suh, H. C. Kim and C. S. Hong, *Chem.–Eur. J.*, 2011, **17**, 3028.
- L. Bogani, A. Vindigni, R. Sessoli and D. Gatteschi, *J. Mater. Chem.*, 2008, **18**, 4750.
- T. D. Harris, M. V. Bennett, R. Clérac and J. R. Long, *J. Am. Chem. Soc.*, 2010, **132**, 3980.